Atmospheric Research 339 (2026) 109052

Contents lists available at ScienceDirect

Atmospheric Research

journal homepage: www.elsevier.com/locate/atmosres

MJO influences on rainfall diurnal cycle during boreal summer over Peninsular Malaysia

Afiqah Bahirah Ayoub [a], Liew Juneng [a,*], Fredolin Tangang [b,a], Ahmad Fairudz Jamaluddin [c]

[a] Department of Earth Sciences and Environment, Faculty of Science and Technology, Universiti Kebangsaan Malaysia, Bangi, Selangor, Malaysia
[b] Faculty of Arts and Social Sciences, Universiti Brunei Darussalam, Jalan Tungku Link, Brunei Darussalam
[c] National Climate Centre, Malaysian Meteorological Department, Petaling Jaya, Selangor, Malaysia

ARTICLE INFO

Keywords:
Madden-Julian Oscillation
Diurnal cycle
Peninsular Malaysia
Rainfall

ABSTRACT

The influence of the Madden-Julian Oscillation (MJO) in its early phases on the diurnal cycle of rainfall in Peninsular Malaysia during boreal summer was investigated. A composite of daily rainfall revealed noticeable differences among west coast (WC), the Foothills of Titiwangsa (FT), Inland (IN), and the east coast (EC) regions. During the initial MJO phases, there is a tendency for increased (decreased) rainfall probability along WC, FT, and IN (EC). Notably, the most significant variations in precipitation tend to occur in the late afternoon to evening (approximately 1400–2000 Malaysia Standard Time), when sea-breeze convergence and orographic effects organize convection. The peak diurnal rainfall intensity could either double or halve the climatological hourly rainfall mean, especially during Phase 2. Diurnal amplitude changes are quantified using evening dominance over WC and near Titiwangsa Range (FT,IN), while EC exhibits weaker dominance. The MJO's distant effects on Peninsular Malaysia result in alterations to the diurnal rainfall pattern during the early MJO phases when the primary convection centre remains over the Indian Ocean. These conditions create a favourable environment for local convection to dominate due to the weakening of the southwest monsoon wind. Along the west coast, an intensified sea breeze results in enhanced onshore moisture transport that fuels local convection. In contrast, the east coast is drier because opposing sea-breeze and monsoon flows reduce moisture transport toward the northeastern coast. Overall, the MJO modulates the monsoon background, strengthening regional forcing and enhances the west–east coast rainfall contrast.

1. Introduction

The main driver of intraseasonal rainfall variability over Maritime Continent is widely known as the Madden-Julian Oscillation (MJO) (Madden and Julian, 1972). It modulates regional meteorological elements like temperature, wind, and precipitation, while altering the timing and intensity of diurnal cycle of rainfall, and air quality causing substantial variations over the Maritime Continent (Jud et al., 2020; Qian, 2020; Tan et al., 2022; Zelinsky et al., 2019; Zhu and Li, 2023). However, the MJO signal over the Maritime Continent, especially in Peninsular Malaysia is spatially non-uniform. It is strongly modulated by seasonal background circulation, land-sea contrasts, topography, frictional moisture convergence, and land-surface processes (Barrett et al., 2021; Kikuchi, 2020; Li et al., 2020; Zhang and Dong, 2004). This seasonality is important for Peninsular Malaysia because its rainfall is strongly shaped by diurnal cycle driven by land-sea breeze and orographic effects, which can be amplified or suppressed by intraseasonal changes in the large-scale environment.

During boreal summer in Peninsular Malaysia because the MJO signal peaks near the northern hemisphere of the equator, extending from the Bay of Bengal through the South China Sea to the eastern Pacific Ocean (Zhang and Dong, 2004). Its propagation moves northward through the equatorial region by passing through the MC via the South China Sea and the Philippine Sea (Wang and Rui, 1990; Zhang and Ling, 2017). On the other hand, the Boreal Summer Intraseasonal Oscillation (BSISO) is a key feature of subseasonal climate variability that exhibits northward and north-westward propagation during this period (Jiang et al., 2004; Kikuchi, 2020). While the BSISO predominantly propagates in a north-south direction, the MJO is confined to east-west propagation along the equator (Wang et al., 2018). The significant correlation between BSISO1 index and Real-time Multivariate (RMM) highlights the eastward propagation of the MJO (Lee et al., 2013). This difference in

* Corresponding author.
E-mail address: juneng@ukm.edu.my (L. Juneng).

https://doi.org/10.1016/j.atmosres.2026.109052
Received 17 March 2025; Received in revised form 17 March 2026; Accepted 26 April 2026
Available online 27 April 2026

propagation patterns results in each phenomenon influencing tropical weather in distinct ways.

Prior research on the impact of the MJO on rainfall in the Maritime Continent has primarily focused on boreal winter due to the higher frequency of strong MJO signal days during this period (Zhang and Dong, 2004; Zhou et al., 2022; Zhu and Li, 2023). Nevertheless, wet rainfall anomalies observed during suppressed-to-transition stages over the Maritime Continent (Phases 1 to Phase 3) (Birch et al., 2016; Da Silva and Matthews, 2021; Lim et al., 2017). Over the western Maritime Continent, the diurnal cycle of rainfall increases (decreases) during the early (late) intraseasonal phases (Lu et al., 2019; Oh et al., 2012). Rainfall tends to peak over land before the arrival of active convection and shift offshore as the convective envelope becomes established over the Maritime Continent (Birch et al., 2016; Zhou et al., 2022). Although boreal summer generally exhibits weaker convective amplitude than boreal winter over the Maritime Continent, the timing of the diurnal rainfall peak remains unchanged (Marzuki et al., 2024). However, despite evidence of the wet anomalies and diurnal cycle modulation over the broader Maritime Continent, the regional characteristics and physical mechanisms during boreal summer remain poorly understood over Peninsular Malaysia. This knowledge gap is important because rainfall over Peninsular Malaysia is strongly influenced by coastal contrasts (Strait of Malacca and South China Sea), complex terrain, and mountain-valley circulation (Fujita et al., 2010; Jamaluddin et al., 2019; Tan et al., 2022). Therefore, improving understanding of how boreal-summer MJO phases modulate the diurnal rainfall cycle over Peninsular Malaysia is essential for interpreting sub-seasonal rainfall variability in this region.

This study utilises the RMM index to investigate the impact of the eastward propagation of MJO during its early phases on Peninsular Malaysia, focusing on the diurnal cycle of rainfall and wind circulation during the boreal summer. The paper is organized as follows: Section 2 details the data sources and methodology. The study's results are presented in Section 3, followed by discussions in Section 4. Finally, the summary is provided in Section 5. Overall, this study aims to enhance our understanding of how the early phases of MJO impact local rainfall variability during the boreal summer in Peninsular Malaysia. This contributes to improving the accuracy of subseasonal and seasonal weather forecasts for the region.

2. Data and method

For rainfall datasets, meteorological station data provided by the Malaysian Meteorological Department (MMD) and a gridded dataset from the Global Precipitation Measurement (GPM) Final Precipitation L3 project with a 0.1° horizontal resolution were utilised (Kidd and Huffman, 2011). The observation datasets consist of hourly rainfall measurements from 22 rain-gauge stations located across Peninsular Malaysia (99°E - 105°E, 1°N - 8°N) (Fig. 1). Stations were retained if data completeness exceeded 98%, and missing values were preserved in the original dataset and treated as missing during the analysis. Hourly rainfall data were analysed to assess diurnal-scale variations. In this study, gridded datasets were included due to the limited availability and sparse distribution of hourly station data for climate simulations. Therefore, gridded data were utilised to observe broader spatial distributions of rainfall anomalies over both land and ocean. The daily observation data represent accumulated 24-h data for a period commencing at 0800 Malaysia time, corresponding to +0 UTC in the recorded gridded data. To assess the reliability of the gridded dataset, 106 daily station data points were plotted alongside GPM data to compare patterns, as detailed in Section 3.1. Peninsular Malaysia was subdivided into four distinct sub-regions: West Coast (WC) (n = 6), Foothill of the Titiwangsa Range (FT) (n = 5), Inland (IN) (n = 5), and East Coast (EC) (n = 6) (Jamaluddin et al., 2019) (Fig. 1). This subdivision was adopted to account for the strong regional modulation of the diurnal rainfall cycle over Peninsular Malaysia. The latitude-longitude

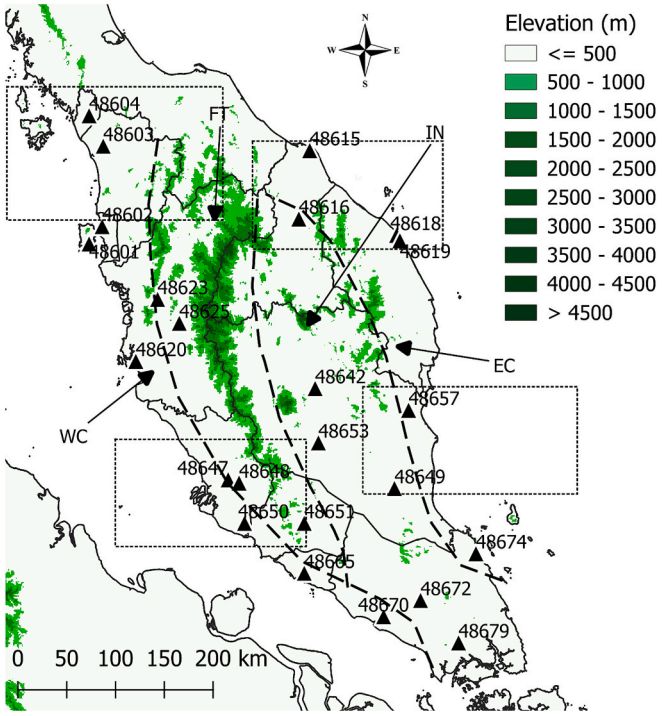

Fig. 1. Topography of Peninsular Malaysia and location of 24 rain-gauge station data. The rectangular dotted show the area for vertical profile of moisture flux divergence at 99.5°E-101.5°E and 5° N - 6.75°N, 100.5°E-102.5°E and 2.5° N – 3.5°N, 101.75°E-103.5°E and 5.25° N – 6.25°N, and 102.75°E-104.75°E and 3° N – 4°N.

Table 1
Location and elevation of twenty-four rain gauge data station across Malaysia.

Station ID	Station Name	Latitude (°)	Longitude (°)	Elevation (m)
West Coast (WC)				
48,601	Bayan Lepas	5.30	100.27	2.8
48,602	Butterworth	5.47	100.38	2.8
48,603	Alor Setar	6.20	100.40	3.9
48,604	Chuping	6.48	100.27	21.7
48,620	Sitiawan	4.22	100.70	7.0
48,650	KLIA Sepang	2.73	101.70	16.3
48,665	Malacca	2.27	102.25	8.5
48,670	Batu Pahat	1.87	102.98	6.3
Foothills of Titiwangsa (FT)				
48,623	Lubok_Merbau	4.80	100.90	77.5
48,625	Ipoh	4.57	101.10	40.1
48,647	Subang	3.12	101.55	16.5
48,648	Petaling Jaya	3.10	101.65	60.8
48,651	Kuala Pilah	2.73	102.25	144.0
Inland (IN)				
48,642	Batu Embun	3.97	102.35	59.5
48,649	Muadzam Shah	3.05	103.08	33.3
48,653	Temerloh	3.47	102.38	39.1
48,672	Kluang	2.02	103.32	88.1
48,679	Senai	1.63	103.67	37.8
East Coast (EC)				
48,615	Kota Bharu	6.17	102.28	4.6
48,616	Kuala Krai	5.53	102.20	68.3
48,618	Kuala Terengganu_Airport	5.38	103.10	5.2
48,619	K.K.Terengganu	5.33	103.13	5.33
48,657	Kuantan	3.78	103.22	15.3
48,674	Mersing	2.45	103.83	43.6

coordinates and elevations of these stations are provided in Table 1.

The Real-time Multivariate index (RMM) developed by Wheeler and Hendon (2004) is a widely used indicator in numerous research studies. The RMM is designed to define the phase and amplitude of the MJO by projecting daily anomaly data onto the two-leading pairs of empirical orthogonal functions (EOFs) derived from the combination of Outgoing Longwave Radiation (OLR), 850-hPa zonal winds, and 200-hPa zonal winds, equatorially averaged over 15°S to 15°N. MJO days are considered in the calculation when the amplitude is higher than 1.0. This study utilised the RMM by the Bureau of Meteorology Australia (BOM) to track MJO (available at http://www.bom.gov.au/climate/mjo).

The analysis covers approximately 18 years (2001–2018) across all datasets and focuses on the 3-months of boreal summer (June–July–August). This period was selected based on the availability of quality controlled hourly rain-gauge observations over Peninsular Malaysia to ensure a uniform and directly comparable analysis between station observations and gridded datasets. A rainy day is defined as a day with at least 1 mm of rainfall. The significance of MJO modulations in terms of the probability of a rainy day for each MJO phase was assessed. The probability of a rainy day at each station was averaged within subregions for each phase. Intraseasonal variations in rainfall were examined by calculating anomalies for the early phases of the MJO using the RMM index. Rainfall anomalies were calculated for both daily and hourly rainfall data depending on the analysis. These anomalies were obtained by subtracting the corresponding JJA climatological mean (daily or hourly) from the observed rainfall for each phase. The seasonal climatological mean was calculated by averaging the rainfall values for boreal summer over the entire period. Subsequently, composite mean rainfall anomalies were created by averaging rainfall anomalies across Phase 1 to Phase 4. The statistical significance of the rainfall composites was evaluated using a Monte Carlo resampling method (Wilks, 2011). This random sampling was repeated 300 times to obtain robust estimations, and the results were assessed at the 5% significance level using a two-sided test.

To observe variations in regional air movement, a comprehensive dataset of wind circulations, moisture flux divergence, specific humidity, and air temperature were obtained from the fifth generation of the European Centre for Medium-Range Weather Forecasts (ECMWF) Reanalysis, known as ERA5 (Hersbach et al., 2020). The analysis focuses on the lower troposphere (1000–800 hPa), which directly controls moisture transport and convective convergence, and the mid-upper troposphere (800–100 hPa) to characterise large-scale modulation of the atmospheric column. To assess thermodynamic conditions, composite temperature anomalies were analysed alongside moisture flux divergence to identify phase-dependent changes in atmospheric stability and the land-sea thermal contrast associated with diurnal rainfall variability. In addition, to examine changes in atmospheric circulation, the hourly composite vertical profile of moisture flux divergence was analysed at 99.5°E-101.5°E and 5° N - 6.75°N, 100.5°E-102.5°E and 2.5° N – 3.5°N, 101.75°E-103.5°E and 5.25° N – 6.25°N, and 102.75°E-104.75°E and 3° N – 4°N was analysed (Fig. 1).

3. Result

3.1. MJO impact on daily rainfall

The results indicate that anomalous daily rainfall and 850-hPa wind patterns across Peninsular Malaysia are strongly associated with MJO phases (Fig. 2). Distinct daily rainfall patterns emerge along the west and east coasts of Peninsular Malaysia for each phase. In Phase 1, dry conditions are observed in parts of the northeastern Peninsular Malaysia, while the west coast experiences notably wetter conditions. Progressing to Phase 2, significantly wetter conditions are recorded across the west coast, contrasting with drier conditions along the northern east coast. Additionally, prevailing easterly anomalies dominate Peninsular Malaysia and its surrounding areas during the early phases, indicating a weakening of the southwesterly monsoonal wind (Fig. 2b). Comparatively, during boreal winter during Phases 1 and 2 are characterised by drier conditions across Peninsular Malaysia (Da Silva and Matthews, 2021; Lim et al., 2017). This highlights the seasonal differences in eastward-propagating MJO-associated weather conditions between boreal summer and winter in Peninsular Malaysia.

During phase 3, wet rainfall anomalies across Peninsular Malaysia begin to diminish over land while remaining dominant over the surrounding seas, resulting in fewer stations with significant rainfall anomalies across the peninsula. A northwesterly wind flow crosses Peninsular Malaysia toward its southern region, with stationary wind patterns are observed over the South China Sea near the northeastern coast of the peninsula. Rainfall anomalies are generally higher over the ocean than over land. By Phase 4, weather conditions over Peninsular

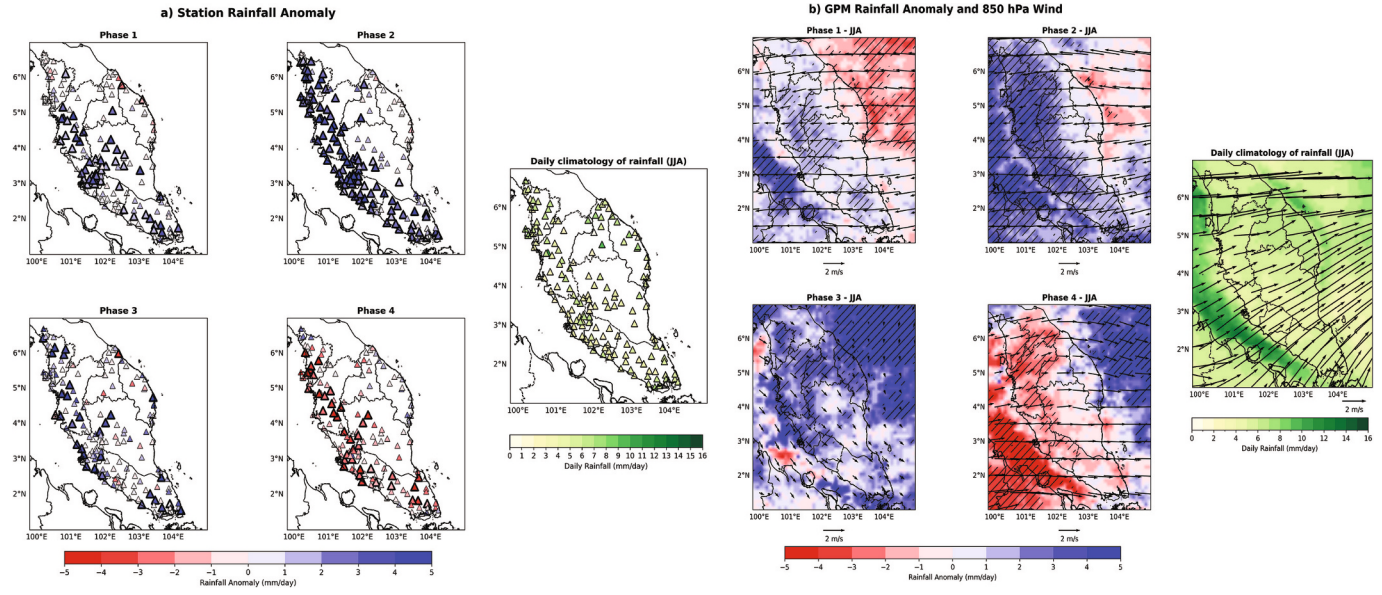

Fig. 2. a) Composites of daily station rainfall anomaly (mm/day) and for Phase 1 to Phase 4 and daily climatology rainfall over the Peninsular Malaysia, significant value with bold triangle and b) Composites of daily GPM rainfall anomaly (mm/day) and wind at 850-hPa (m/s) for Phase 1 to Phase 4 and daily climatology rainfall over the Peninsular Malaysia, significant value with shaded area.

Malaysia shift, with drier conditions on the west coast and wetter conditions along the east coast. The westerly wind anomaly intensifies the southwesterly monsoonal wind from Sumatra, crossing Peninsular Malaysia toward the South China Sea. Overall, the impact of the MJO is more pronounced along the west coast than on the east coast across most phases. The patterns of significant values between station data and the gridded dataset align closely, suggesting that the gridded dataset is suitable for further analysis of the diurnal cycle, as discussed in the next section.

The probability of rainy days in the West Coast (WC) region increases by approximately 1.38% in Phase 1, 10.93% in Phase 2, and 8.4% in Phase 3 compared to the boreal summer (JJA) baseline (See Fig. 3.). In Phase 4, this probability decreases by about 2.82%. Moving toward central Peninsular Malaysia, stations in the Foothill of Titiwangsa Range (FT) and Inland (IN) regions show a similar pattern, with increased probabilities for rainy days during the early phases. Both FT and IN regions experience increases of around 4.28% to 4.44% in Phase 1 and notable rises of approximately 9% to 11% in Phase 2, with FT showing slightly higher values than IN. In Phase 3, IN records a 5.1% increase in rainy days, while FT shows a smaller increase of 3.96%. Both regions then exhibit a decline in the probability of rainy days in Phase 4, ranging from 7.98% to 8.46%. In contrast to the other regions, the East Coast (EC) shows a decrease in the probability of rainy days from Phase 1 (−2.39%) to Phase 2 (−0.41%). This trend reverses in the later phases, with an increase of 3.24% in Phase 3 and a slight rise of 0.43% in Phase 4. These results show a phase dependent shift in where rainy-day probability is enhanced, with the strongest increases concentrated over WC, FT, IN in Phases 1–2 (peaking in Phase 2), while the EC becomes wetter later (Phase 3–4). This pattern is consistent with the propagation MJO as the convective envelope approaches the Maritime Continent. As a robustness check, the daily rainfall composites were also recomputed separately for El Niño-Southern Oscillation (ENSO) years (not shown). Additional composites stratified by ENSO phase (not shown) indicate that the main phase-dependent spatial rainfall anomaly patterns remain qualitatively consistent across ENSO conditions. ENSO primarily affects the magnitude of the anomalies rather than the overall spatial pattern.

3.2. MJO impact on diurnal cycle

In addition to the significant differences in rainfall diurnal patterns associated with MJO phases, notable variations were observed in evening rainfall, which tended to occur between 1400 MST and 2000 MST, especially over FT and IN (Fig. 4 (b,c)). In contrast, a negative rainfall anomaly was recorded over the EC during the same period (Fig. 4(d)). For the WC, the rainfall anomaly was most pronounced in the early morning from 0100 MST to 0400 MST. Compared to the climatological hourly average rainfall, the anomaly during the early MJO phases can either increase or decrease the diurnal rainfall peak by up to twice the normal amount. According to Joseph et al. (2008), the heightened

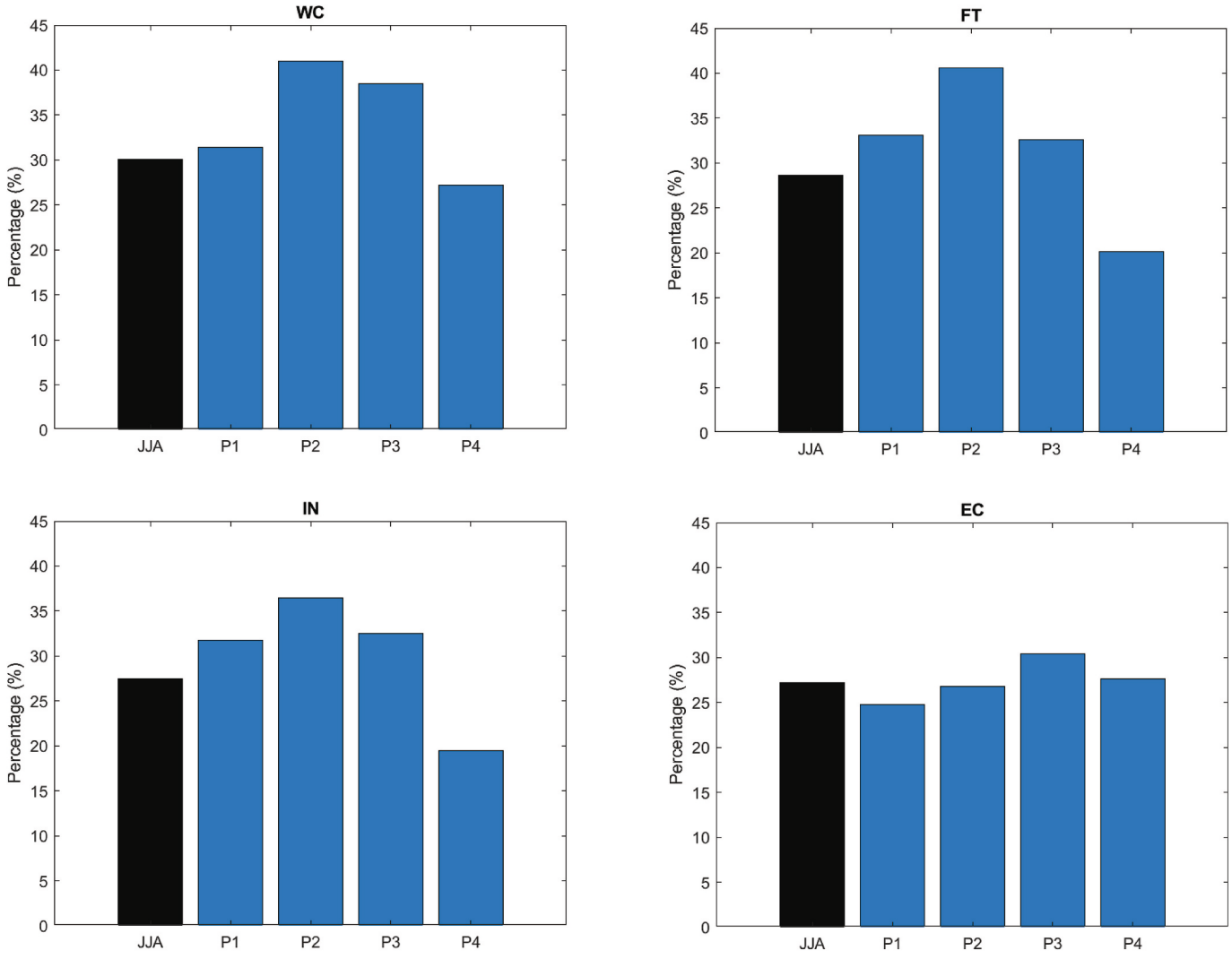

Fig. 3. The probability for rainy days (%) for four sub-regions during Phase 1 to Phase 4 compared it to boreal summer (JJA).

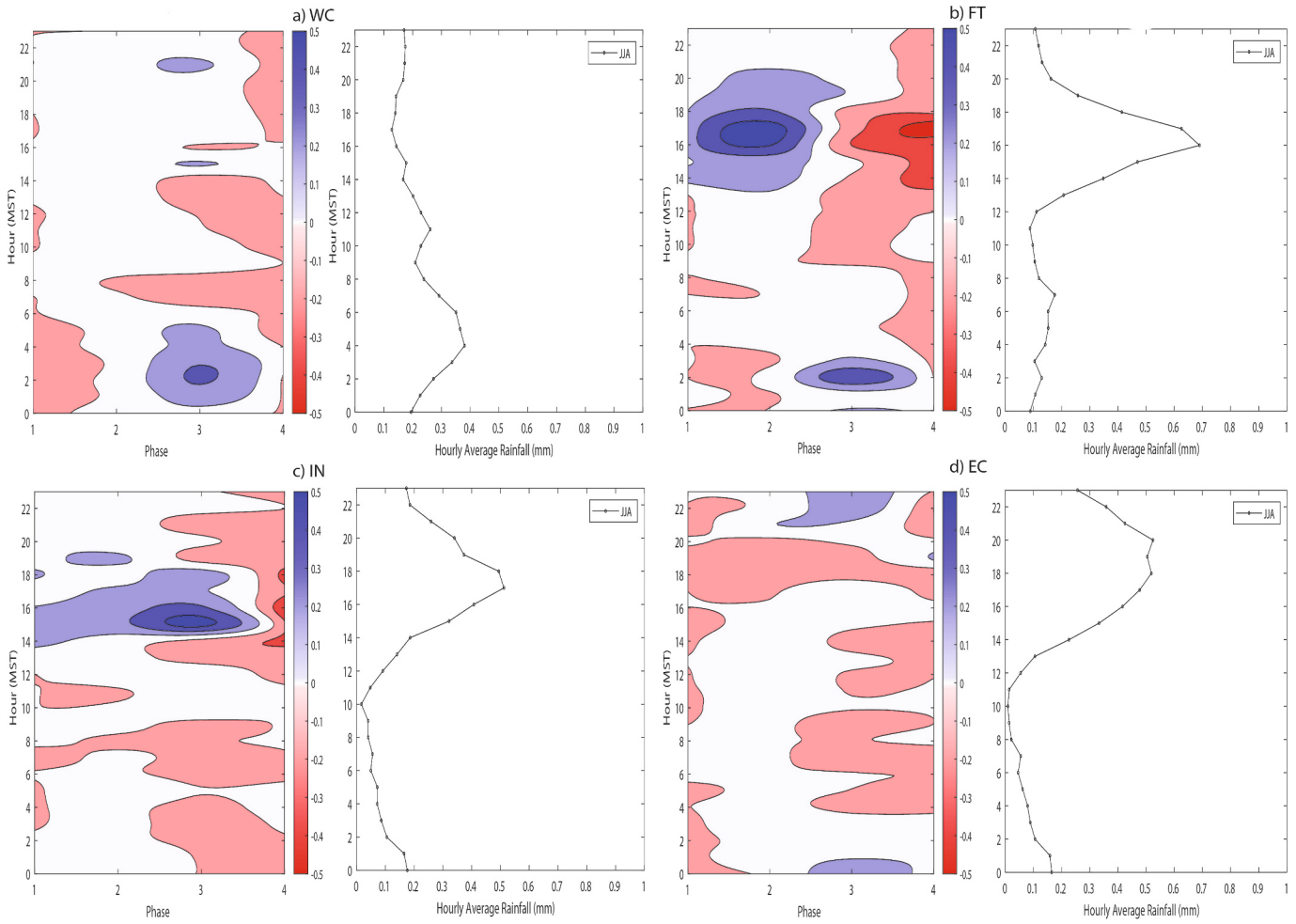

Fig. 4. The anomaly (mm/h) of the rainfall diurnal cycle of the MJO phases (shaded), rainfall intensity climatology for JJA (curves; mm/h) over the a) WC, b) FT, c) IN, and d) EC. Rainfall intensity climatology for JJA is smoothed with 3-hourly running mean.

convective activity in the afternoon can be attributed to the convergence of sea breeze and crosswinds emerging from gaps in the Titiwangsa Range highlands. The interaction of sea breezes from the west, east and the southern part of the east coast further enhances afternoon convection. The narrowness of the peninsula and the absence of mountain ranges in the southern region of Peninsular Malaysia (Fig. 1) increase the likelihood of collisions between the west coast and east coast breezes. This pattern of increased rainfall along the west coast of Peninsular Malaysia is also observed during the inter-monsoon period.

To quantify the influence of intraseasonal variability on the amplitude of the diurnal cycle rainfall, we computed the normalized relative amplitude (NRA) (Rauniyar and Walsh, 2011) (Table 2). NRA defined as the mean rainfall during 0000–1100 MST minus that during 1200–2300 MST, normalized by the JJA climatological mean rainfall. Negative (positive) NRA indicates an evening (morning) dominant rainfall relative to climatology. Overall, the strongest intraseasonal modulation occurs over the western and central region (WC, FT, IN). Over WC, NRA is negative in Phase 1–2 (−0.209, −0.174) and turn positive in Phase 3–4 (0.351, 0.069), indicating a shift from evening to morning dominant rainfall. Over the regions near the Titiwangsa Range (FT, IN), NRA is strongly negative during Phases 1–2, ranging from −0.537 to −1.191 in FT and from −0.708 to −0.584 in IN. This indicates a strong enhanced evening dominance. In later phases, FT becomes positive in Phase 3–4 (0.566, 0.839). Meanwhile IN remains negative through Phase 3 (−0.739) before shift to positive in Phase 4 (0.856), coincident with suppressed evening rainfall (−0.155 mm/h) and near zero morning anomalies (0.002 mm/h). In contrast, EC shows weaker modulation, with small NRA values with positive in Phase 1 and Phase 4 (0.139, 0.308) and slightly negative in Phase 2–3 (−0.044, −0.122). Overall, the

Table 2
Composite hourly rainfall anomalies relative to the seasonal climatology for WC, FT, IN, and EC during selected phases. For each region and phase, the table lists the average evening anomaly (12–23 MST), average early-morning anomaly (00–11 MST), and the normalized diurnal amplitude. The positive (negative) NRA indicates a stronger morning (evening) dominance of rainfall relative to climatology.

Region	Phase	Evening anomaly (12–23 MST) (mm/h)	Morning anomaly (00–11 MST) (mm/h)	Normalized Relative Amplitude (NRA)
WC	1	0.015	−0.031	−0.209
	2	0.108	0.069	−0.174
	3	0.071	0.150	0.351
	4	−0.062	−0.047	0.069
FT	1	0.136	0.022	−0.537
	2	0.280	0.026	−1.191
	3	0.002	0.123	0.566
	4	−0.191	−0.013	0.839
IN	1	0.137	0.006	−0.708
	2	0.146	0.039	−0.584
	3	0.131	−0.004	−0.739
	4	−0.155	0.002	0.856
EC	1	−0.042	−0.013	0.139
	2	0.042	0.033	−0.044
	3	0.070	0.044	−0.122
	4	−0.048	0.016	0.308

diurnal cycle amplitude is strongly modulated over WC and the regions near Titiwangsa Range (FT, IN), while changes over EC are comparatively weak.

The differences in rainfall anomaly peaks between the sea and land can be observed in the morning (0200 MST) and late evening (1800 MST) using the GPM rainfall dataset (Fig. 5). Climatological patterns indicate that rainfall predominantly occurs over the ocean during the early morning, particularly in the Strait of Malacca. By late evening, rainfall shifts to land areas across Peninsular Malaysia, with heavy rainfall concentrated in the northeastern part of the region. During the early phases of the MJO, the rainfall anomaly peak is observed in the morning over the Strait of Malacca, while the evening anomaly peak covers the west coast and inland areas of Peninsular Malaysia. In contrast, reduced rainfall is observed in the northern part of the east coast, including adjacent areas of the South China Sea. In phase 3, the early morning rainfall anomaly peaks in the northwest of the region. Meanwhile, in the evening, the rainfall anomaly becomes more dispersed with less rainfall observed throughout Peninsular Malaysia. As the MJO progresses into Phase 4, wet and dry conditions show distinct patterns that differ from those in the earlier phases of the MJO.

Heavy rainfall along the west coast of Peninsular Malaysia is correlated with the prevailing wind pattern (Jamaluddin et al., 2019; Joseph et al., 2008). Although minor discrepancies exist due to differences in gridded data resolution, the diurnal variation in rainfall (Fig. 5) closely mirrors the temporal evolution of low-level moisture flux divergence (Fig. 6). The climatological maximum convergence and wind patterns exhibit an eastward movement toward the east coast region, particularly in the evening. The planetary boundary layer becomes unstable due to solar heating at the surface and in the atmosphere, with this instability peaking during the day and causing maximum convergence near the Titiwangsa Range in the afternoon.

During the early phases of the MJO, particularly in Phase 2, convergence and divergence are unstable near the Titiwangsa Range. More substantial convergence anomalies with slower wind speeds occur along the west coast. Additionally, northeasterly anomaly winds weaken the climatological southwesterly winds. As a result, the diurnal peak becomes prominent in the late evening across most parts of west coast of Peninsular Malaysia. In Phase 3, in the morning, the strong convergence in the northern part of the west coast, and strong divergence in the central part of the west coast near the Strait of Malacca result in a positive rainfall anomaly across much of the northwest coast. By the evening, strong and unstable divergence near the Titiwangsa Range weakens the climatological pattern. In Phase 4, the remaining low divergence near the eastern side of the Titiwangsa Range along with westerly winds transporting moisture away, resulting the in drier-than-normal conditions across Peninsular Malaysia.

Fig. 7 shows composite temperature anomalies over Peninsular Malaysia in JJA for Phase 1–4 at 0200 MST and 1800 MST, together with the JJA climatology. In Phase 1 and 2, cooler than normal conditions at 0200 MST are apparent over the peninsula. This is consistent with enhanced nocturnal cloudiness and nearby convective activity over nearby. By 1800 MST, the negative temperature anomalies are concentrated over the coastal of west coast and Strait of Malacca (peak at Phase 2). In contrast, relatively warmer anomalies along parts of the east coast suggest reduced cloud cover and weaker convective cooling compared with the west coast. This further emphasizes the different between west and east coast anomalies. During Phase 3, negative anomalies remain widespread over Peninsular Malaysia from 0200 to 1800 MST. This indicates generally cooler land conditions and a weaker land-ocean thermal contrast. By Phase 4, temperatures become warmer than normal over land at 0200 MST, and by 1800 MST the warm anomalies extend offshore. This indicates that a reduced cloud cover and supressed convective cooling overall.

4. Discussion

During boreal summer, the impact on rainfall in Peninsular Malaysia appears to be more significant during the early suppressed phases associated with the eastward-propagating MJO than during the active MJO phases. The early MJO phases lead to two distinct weather patterns: i. wet conditions across most areas of Peninsular Malaysia, particularly along the west coast, and ii. dry conditions in the northern part of the east coast region (Fig. 2). Our analysis reveals that the rainfall anomaly can either increase or decrease by up to twice the

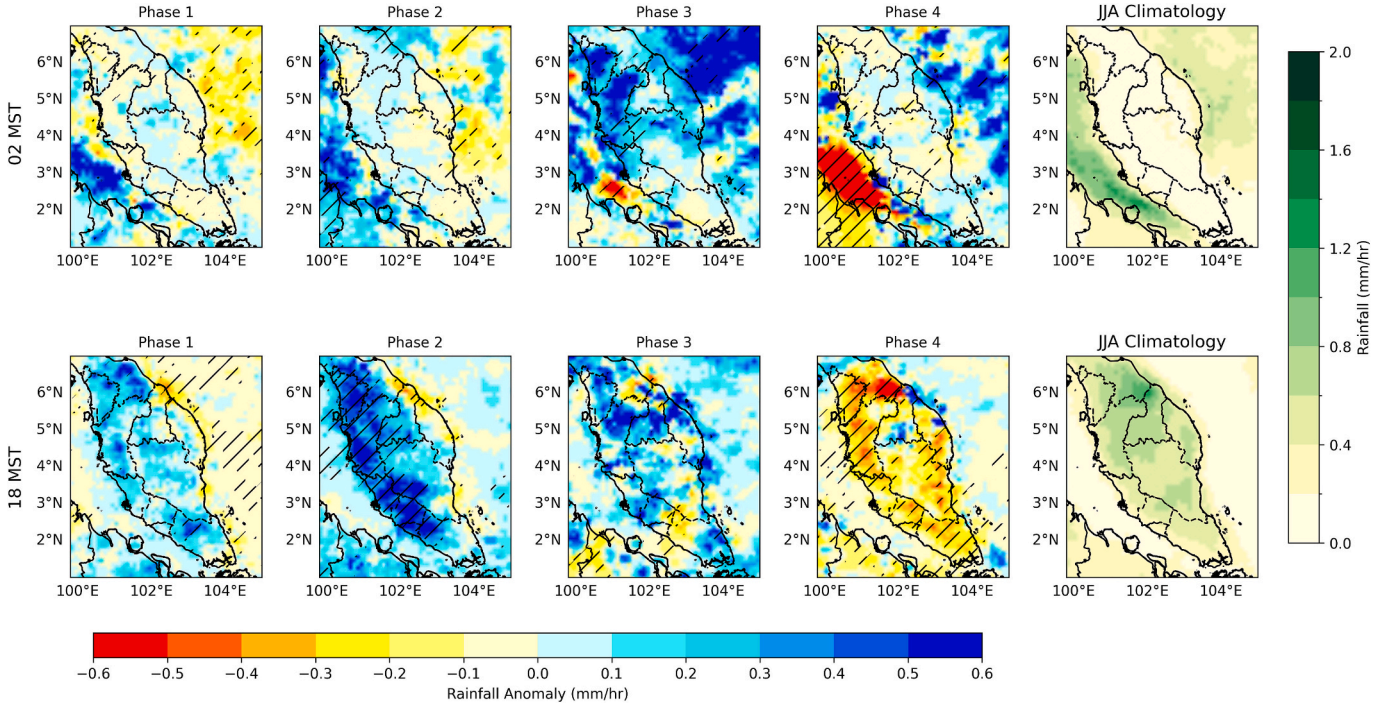

Fig. 5. The anomaly (mm/h) of the rainfall diurnal cycle at 0200 MST and 1800 MST using GPM datasets for Phase 1 to Phase 4 and JJA climatology.

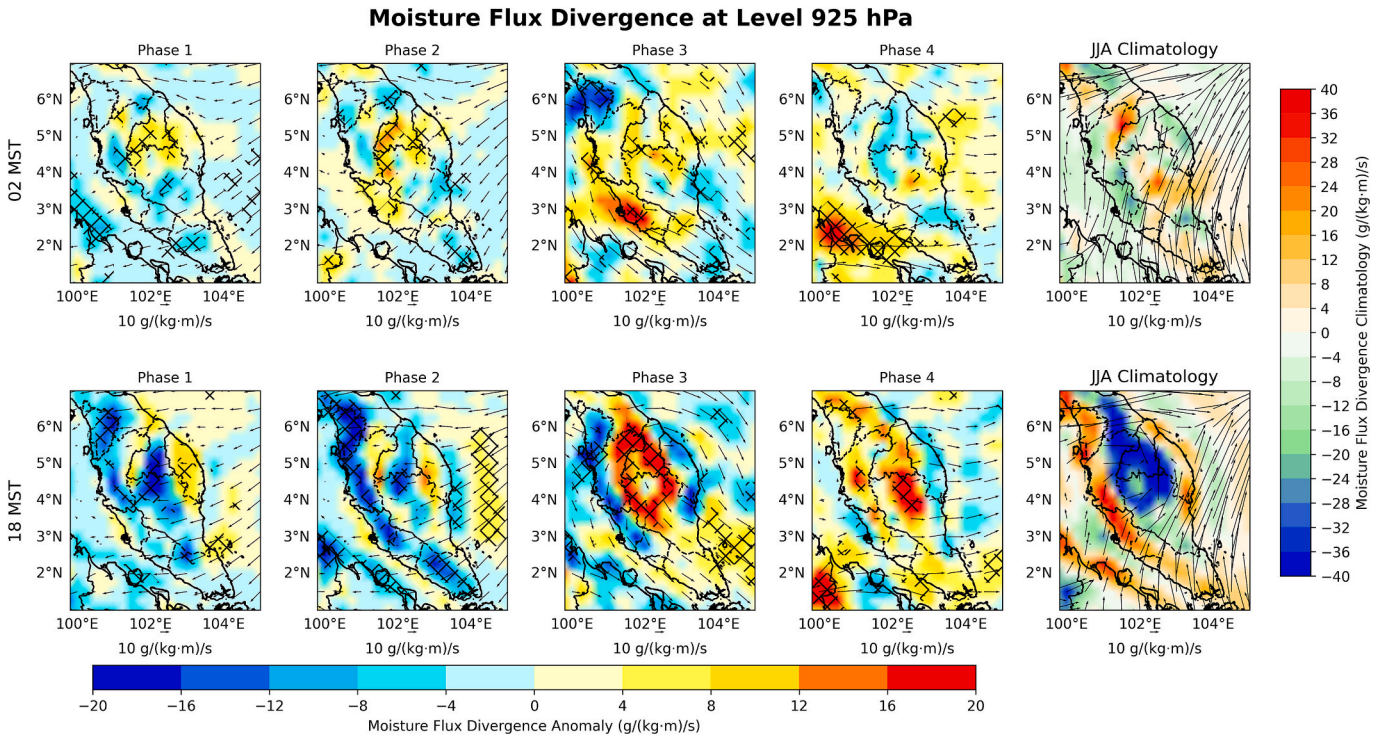

Fig. 6. MJO composites anomaly of 925-hPa moisture flux divergence and wind vectors (unit: g/(kg·m)/s) with significant value at 95% (shaded) at 0200 MST and 1800 MST.

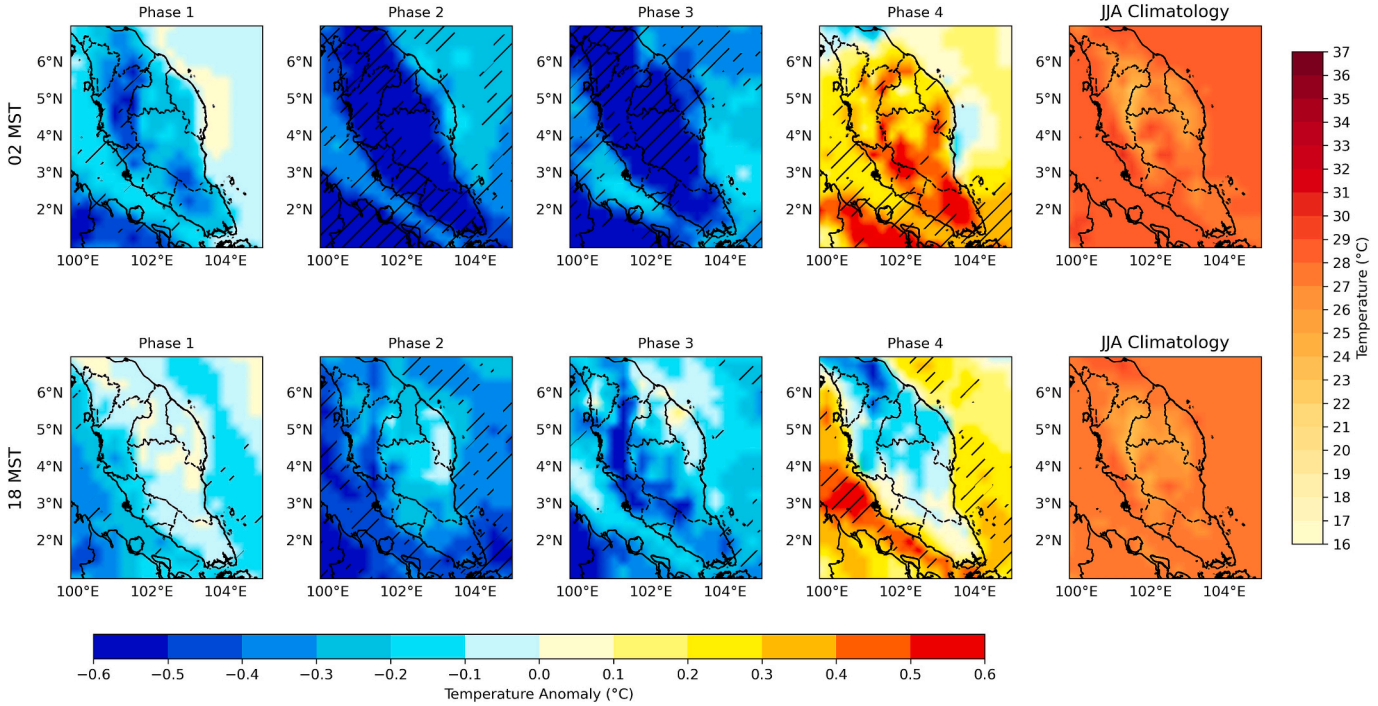

Fig. 7. MJO composites anomaly of temperature (unit: °C) with significant value at 95% (shaded) at 0200 MST and 1800 MST.

climatological mean during the late evening rainfall peak (Fig. 4). This diurnal modulation is quantified by the normalized relative amplitude (NRA) (Table 2), which shows the strongest phase dependence over WC and the regions near the Titiwangsa Range (FT and IN), with evening-dominant rainfall, especially in Phase 2. In contrast, EC exhibits weak NRA, with a smaller shift from morning to evening rainfall. The discussion will further examine the diurnal cycle variations during the early suppressed phases of the MJO (Phases 1 to 3) and the active MJO phase (Phase 4) in Peninsular Malaysia. Additionally, differences in the diurnal cycle between the west and east coast regions will be explored.

In this study, the "regional effects" refer to the coastal and topographic controls that shape the diurnal cycle of rainfall (sea-land breezes, coastal exposure to the Strait of Malacca and South China Sea, and the Titiwangsa Range). The MJO acts as primarily as a large-scale

modulator by altering the background monsoonal flow and thermodynamic environment, thereby strengthening or suppressing the regional diurnal response. The southwesterly monsoonal wind plays a crucial role in enhancing the sea breezes during boreal summer in Peninsular Malaysia. The oscillations in the local sea breeze are responsible for changes in the maximum diurnal rainfall peak during various MJO phases. The collision between anomalous high-speed sea breezes and gap flows from mountainous areas leads to a significant increase in rainfall from the afternoon to late afternoon across the region. Consistent with the rainfall behaviour, the composite temperature anomalies show cooler-than-normal conditions during Phases 1–3 (especially Phase 2), indicating stronger convective cloudiness. Meanwhile, Phase 4 shifts to warmer anomalies, indicating suppressed convective over land. Further evidence was provided by analysing the vertical profile of moisture flux divergence over the west coast, divided into various sections, as follows: i. 99.5°E – 101.5°E averaged at 5°N – 6.75°N, and ii. 100.5°E – 102.25°E averaged at 2.5°N – 3.50°N (Fig. 8). Similarly, for the east coast, the selected areas were: i. 101.75°E – 103.5°E averaged at 5.25°N – 6.25°N, and ii. 102.75°E – 104.75°E averaged at 3.0°N – 4.0°N (Fig. 9). The study examined horizontal moisture flux patterns between 1000 hPa and 100 hPa at 0200 MST and 1800 MST. The vertical profile of specific humidity anomalies demonstrates that the local sea-land breeze plays an important role during Phase 1 to Phase 4 of the MJO in Peninsular Malaysia (Fig. 10).

On the west coast, the JJA climatology represents the general pattern of moisture flux divergence during the early morning when atmospheric stability is typically higher. This stability often results in mild moisture convergence near the surface and minimal divergence aloft. The concentrated convergence flux closer to the low-level atmosphere near the ocean indicates less moisture accumulation over the land. By late evening, the climatology shows pronounced moisture convergence at low-level due to peak heating supported by the divergence aloft directed toward the land. This pattern reflects the influence of land heating and the inland movement of oceanic moisture during the evening.

In the early morning of Phase 1 and Phase 2, the atmospheric stability with minimal anomalous divergence near surface facilitates moisture accumulation away from the land. However, in the late evening of Phase 1, moderate low-level anomalous convergence and

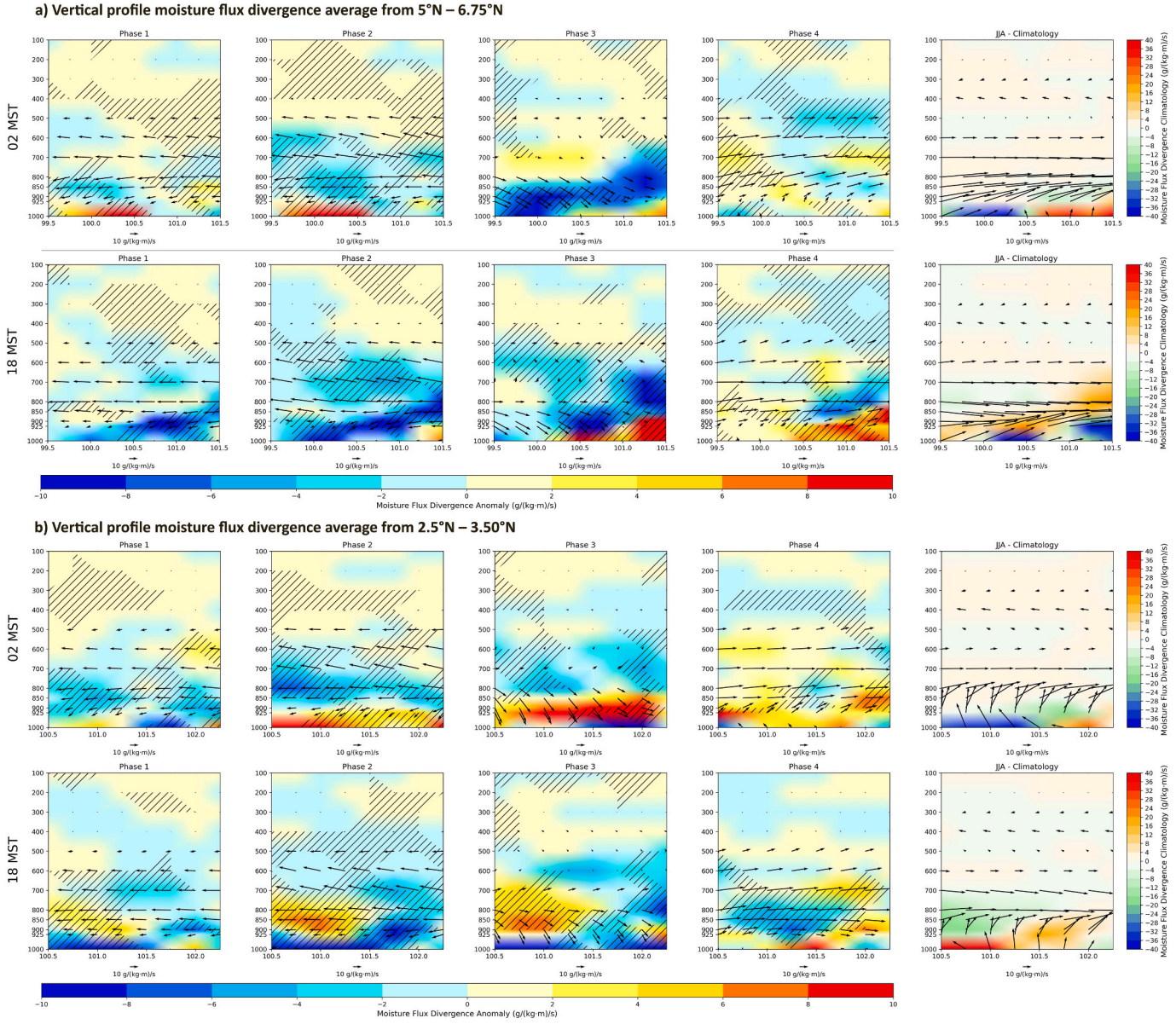

Fig. 8. Vertical profile of moisture flux divergence from 1000 hPa to 100 hPa at west coast Peninsular Malaysia at a) 99.5°E – 101.5°E averaged at 5°N – 6.75°N, and b) 100.5°E – 102.25°E averaged at 2.5°N – 3.50°N with significant value at 95% (shaded) at 0200 MST and 1800 MST.

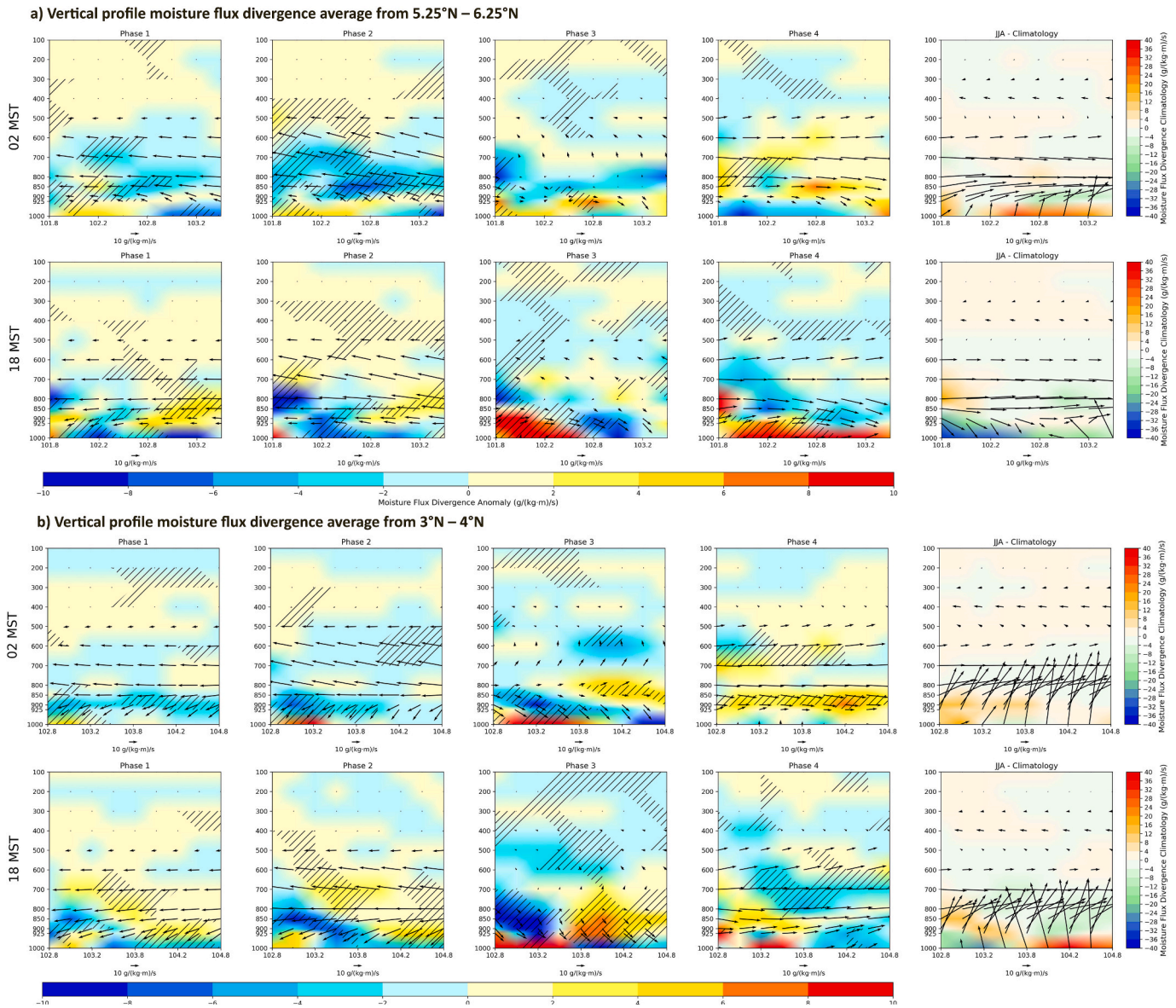

Fig. 9. Vertical profile of moisture flux divergence from 1000 hPa to 100 hPa for east coast Peninsular Malaysia at a) 101.75°E – 103.5°E averaged at 5.25°N – 6.25°N, and b) 102.75°E – 104.75°E averaged at 3.0°N – 4.0°N with significant value at 95% (shaded) at 0200 MST and 1800 MST.

minimal anomalous upper-level divergence create conditions for moderate convective potential along the west coast. In Phase 2, the interaction between monsoonal and anomalous winds, along with the opposing interaction between anomalous surface-level convergence and significant anomalous divergence aloft, combined with climatological surface divergence and low-level convergence, supports more intense evening convection and a pronounced onset of convective activity. During the early morning Phase 3, peak convective activity in the northwest region is driven by strong anomalous surface to low-level convergence, with wind directed toward land which create a favourable condition to sustain convective energy overnight, indicating readiness for an active convective cycle. Meanwhile, in the central west coast, strong anomalous low-level divergence interacting with climatological low-level convergence enhances upward transport moisture. By Phase 4, a gradual decline in activity with slightly more energy present in late evening than in the morning is observed. This pattern aligns with the daily heating cycle leading to reduced convective energy at night.

On the east coast, the southwesterly sea-land breeze during boreal summer winds is stronger compared to that on the west coast. At 0200 MST, divergence dominates at low levels offshore and extends from low to mid-levels over land. This indicates limited near-surface moisture accumulation and reduced upward moisture supply. The moisture divergence flux levels over land areas are slightly higher than those on the west coast, potentially indicating a stronger diurnal influence in the region. At 1800 MST, the northeast region exhibits strong moisture convergence near the surface driven by daytime heating over land. The surface winds indicate flow that is either inland-directed or coast-parallel, implying that moisture is transported toward the coastal zone and supports cloud formation and rainfall. Meanwhile, near the southeast coast, low-level winds show strong divergence near land, indicating that moisture is not accumulating at the surface but is instead transported away, resulting in reduced surface rainfall. This contrasts with the west coast, where low-level convergence is more frequently observed during the evening, supporting moisture accumulation and enhanced rainfall. The modulation of the local sea breeze over the west coast region was consistent with previous studies (Qian, 2008; Qian et al., 2013).

In Phase 1, moisture flux slightly increases compared to the JJA climatology, with a modest rise in anomalous divergence near the surface at 0200 MST. By 1800 MST, the interaction between monsoonal and

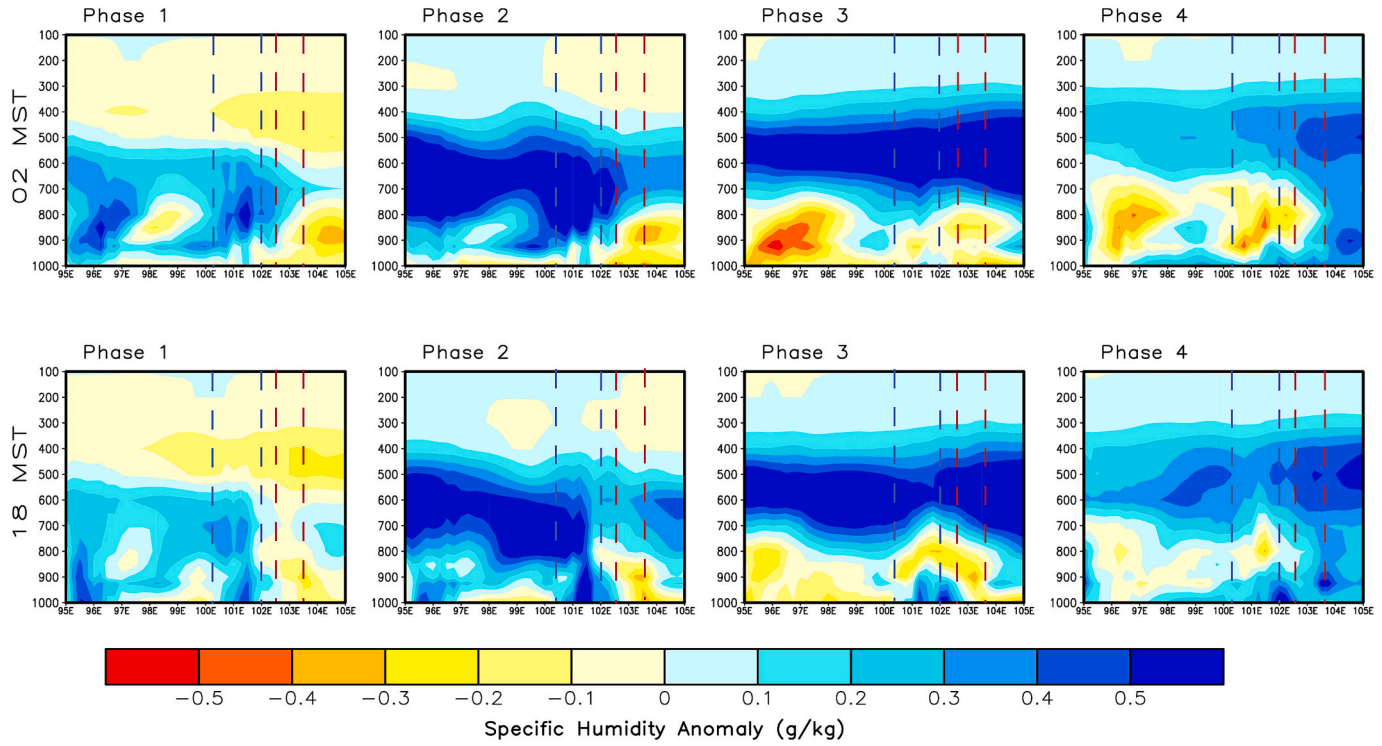

Fig. 10. Vertical profile of specific humidity anomalies (g/kg) for 4 phases of MJO averaged at 5.0°N – 5.75°N from 95°E to 105°E. The blue dotted indicated west coast region (100.25°E – 102°E) and red dotted indicated east coast region (102.5°E – 103.5°E). (For interpretation of the references to colour in this figure legend, the reader is referred to the web version of this article.)

anomalous winds along with mild moisture convergence near the surface and low-level divergence limits the upward transport, reflecting a weaker pattern. During Phase 2, high anomalous moisture flux divergence over land inhibits cloud formation, reducing rainfall over the east coast. As a result, the east coast receives less rainfall compared to the west coast which experiences wetter conditions. In Phase 3, land cooling stabilises conditions, reducing upward moisture flux and supporting a low-level offshore flow. This movement transports residual moisture from land to ocean resulting in limited precipitation over land at 0200 MST. By 1800 MST, daytime heating over land triggers strong convection, drawing moist air from the ocean toward land at lower levels. Rising moisture then diverges back to the ocean at low to mid-level forming a convective loop that supports rainfall over land while redistributing moisture offshore. In Phase 4, the anomalous moisture flux divergence profile weakens, leading to minimal upward flux and weaker convection However, localized shallow convection can still occur under weak divergence anomalies (Figs. 8–9), and the associated low-level moisture conditions are examined using Fig. 10. In general, the characteristics of the local sea breeze along the east coast are similar to those observed along the west coast. However, observations during the early phases are evident in i. the shallow depth of the sea breeze and ii. the stronger return flow caused by the prevailing monsoonal wind (Fig. 8, Fig. 9). These differences contribute to the contrasting rainfall anomalies between the west and east coasts of Peninsular Malaysia.

The vertical profile of specific humidity anomalies averaged at 5.0°N – 5.75°N from 95°E to 105°E, covering Sumatra to Malaysia, was analysed to assess local and large-scale influences (Fig. 10). In Phase 1, localized positive anomalies indicate wetter conditions from Sumatra to the west coast of Peninsular Malaysia, while negative anomalies suggest drier conditions on the east coast. These anomalies are strongest in the lower troposphere and weaken with altitude suggesting a predominantly regional influence driven by coastal effects, diurnal heating, and land-sea interactions. In Phase 2, positive anomalies intensify over Sumatra and the west coast, while the east coast remains dry at low levels. The vertical extension of positive humidity anomalies indicates a deeper moist layer and enhanced convective potential. However, the anomalies remain spatially limited, indicating that the influence is predominantly regional, with larger-scale variability providing only secondary modulation. By Phase 3, positive anomalies intensify from Sumatra to Peninsular Malaysia, with moisture extending into the mid and upper troposphere, indicating a broader and more sustained presence of moisture. Sumatra remains dry due to local effects, while Peninsular Malaysia moistens through coastal and convective processes. In Phase 3, positive moisture anomalies extend into the mid-troposphere, indicating a deeper moist layer than in Phases 1–2. In Phase 4, the contrast between the west and east coasts becomes evident, with dry conditions on the west coast of Peninsular Malaysia and convective conditions on the east coast. Overall, these results show that moisture anomalies over Peninsular Malaysia evolve systematically from suppressed to transition phases (Phase 1–3), when moistening strengthens and deepens over the peninsula. In the active phase (Phase 4), the maximum moisture shifts toward east coast.

5. Summary

Rainfall anomalies in Peninsular Malaysia are influenced by interaction between large scale intraseasonal forcing associated with eastward-propagating MJO-related and regional controls include southwest monsoon background flow, coastal land-sea breeze circulations, and the orographic influence of Titiwangsa Range. The key contribution of this study is that during boreal summer, the strongest wet modulation of the diurnal cycle occurs in the early suppressed to transition phases (Phases 1–3). In these phases, convection is shifts in both timing and location between the Strait of Malacca/west coast and east coast/ South China Sea, even though the main MJO convective centre remains over the Indian Ocean. In contrast, the diurnal modulation shifts with dry weather over west coast in Phase 4 (active MJO).

A comparison between the west and east coast regions revealed

distinct convective behaviours. During MJO Phases 1–2, Peninsular Malaysia is generally wetter especially along the west coast, while moisture-flux divergence and specific-humidity profiles show enhanced moistening in the west and drier low-level conditions over the east coast. At the same time, the thermodynamic response shows cooler near-surface temperature anomalies during the early phases, consistent with enhanced cloudiness and precipitation-related cooling over the peninsula, with the strongest cooling during Phase 2. The enhanced diurnal cycle modulation is also quantified by normalized relative amplitude (NRA), which shows strongest phase dependence over WC and the regions near Titiwangsa Range (FT,IN) with evening dominant rainfall. These results indicate that local convection along the west coast and the Titiwangsa-adjacent interior is amplified when MJO-related circulation anomalies weaken the southwest monsoon background flow and favour stronger sea-breeze convergence and onshore moisture supply. In Phase 3, regional processes dominated moisture dynamics. Nighttime cooling stabilised the atmosphere, promoting offshore flow, while daytime heating over land triggered convection, drawing moist air from the ocean and sustaining potential rainfall across Peninsular Malaysia. By Phase 4, Peninsular Malaysia experienced a reversal of earlier conditions. The west coast became drier, while some areas in northeastern Peninsular Malaysia experienced wetter conditions. This is primarily due to regional diurnal processes drive the pattern, and the MJO related large scale anomalies modulate its intensity.

CRediT authorship contribution statement

Afiqah Bahirah Ayoub: Writing – original draft, Visualization, Validation, Methodology, Formal analysis, Data curation. **Liew Juneng:** Writing – review & editing, Validation, Supervision, Project administration, Methodology, Investigation, Funding acquisition, Conceptualization. **Fredolin Tangang:** Writing – review & editing, Validation, Supervision, Project administration, Methodology, Investigation, Funding acquisition, Conceptualization. **Ahmad Fairudz Jamaluddin:** Writing – review & editing, Validation, Methodology, Data curation.

Declaration of competing interest

The authors declare that they have no conflict of interest.

Acknowledgements

This work was funded by the LRGS/1/2020/UKM-UKM/01/6/1.

Data availability

Data will be made available on request.

References

Barrett, B.S., Densmore, C.R., Ray, P., Sanabia, E.R., 2021. Active and weakening MJO events in the Maritime Continent. Clim. Dyn. 57, 157–172. https://doi.org/10.1007/s00382-021-05699-8.

Birch, C.E., Webster, S., Peatman, S.C., Parker, D.J., Matthews, A.J., Li, Y., Hassim, M.E. E., 2016. Scale interactions between the MJO and the western Maritime Continent. J. Clim. 29, 2471–2492. https://doi.org/10.1175/JCLI-D-15-0557.1.

Da Silva, N.A., Matthews, A.J., 2021. Impact of the Madden–Julian Oscillation on extreme precipitation over the western Maritime Continent and Southeast Asia. Q. J. R. Meteorol. Soc. 147, 3434–3453. https://doi.org/10.1002/qj.4136.

Fujita, M., Kimura, F., Yoshizaki, M., 2010. Morning precipitation peak over the strait of Malacca under a calm condition. Mon. Weather Rev. 138, 1474–1486. https://doi.org/10.1175/2009MWR3068.1.

Hersbach, H., Bell, B., Berrisford, P., Hirahara, S., Horányi, A., Muñoz-Sabater, J., Nicolas, J., Peubey, C., Radu, R., Schepers, D., Simmons, A., Soci, C., Abdalla, S., Abellan, X., Balsamo, G., Bechtold, P., Biavati, G., Bidlot, J., Bonavita, M., De Chiara, G., Dahlgren, P., Dee, D., Diamantakis, M., Dragani, R., Flemming, J., Forbes, R., Fuentes, M., Geer, A., Haimberger, L., Healy, S., Hogan, R.J., Hólm, E., Janisková, M., Keeley, S., Laloyaux, P., Lopez, P., Lupu, C., Radnoti, G., de Rosnay, P., Rozum, I., Vamborg, F., Villaume, S., Thépaut, J.N., 2020. The ERA5 global reanalysis. Q. J. R. Meteorol. Soc. 146, 1999–2049. https://doi.org/10.1002/qj.3803.

Jamaluddin, A.F., Fredolin Tangang, F.T., Wan Ibadullah, W.M., Liew, J., Yik, D.J., Salimun, E., Dindang, A., Abdullah, M.H., 2019. Klimatologi Hujan Diurnal dan Bayu Laut-Darat di Semenanjung Malaysia. Sains Malaysiana 48, 509–522. https://doi.org/10.17576/jsm-2019-4803-03.

Jiang, X., Li, T., Wang, B., 2004. Structures and mechanisms of the northward propagating boreal summer intraseasonal oscillation. J. Clim. 17, 3726–3738. https://doi.org/10.1175/1520-0442(2004)017<1022:SAMOTN>2.0.CO;2.

Joseph, B., Bhatt, B.C., Koh, T.Y., Chen, S., 2008. Sea breeze simulation over the Malay Peninsula in an intermonsoon period. J. Geophys. Res. Atmos. 113, 1–8. https://doi.org/10.1029/2008JD010319.

Jud, M.A., Juneng, L., Tangang, F.T., Latif, M.T., Chung, J.X., Ahamad, F., 2020. Madden Julian oscillation modulation for surface ozone in Peninsular Malaysia. Atmos. Environ. 233, 117577. https://doi.org/10.1016/j.atmosenv.2020.117577.

Kidd, C., Huffman, G., 2011. Global precipitation measurement. Meteorol. Appl. 18, 334–353. https://doi.org/10.1002/met.284.

Kikuchi, K., 2020. Extension of the bimodal intraseasonal oscillation index using JRA-55 reanalysis. Clim. Dyn. 54, 919–933. https://doi.org/10.1007/s00382-019-05037-z.

Lee, J.Y., Wang, B., Wheeler, M.C., Fu, X., Waliser, D.E., Kang, I.S., 2013. Real-time multivariate indices for the boreal summer intraseasonal oscillation over the Asian summer monsoon region. Clim. Dyn. 40, 493–509. https://doi.org/10.1007/s00382-012-1544-4.

Li, X., Yin, M., Chen, X., Yang, M., Xia, F., Li, L., Chen, G., Yu, P., Zhang, C., 2020. Impacts of the tropical pacific–indian ocean associated mode on madden–julian oscillation over the maritime continent in boreal winter. Atmosphere (Basel) 11. https://doi.org/10.3390/atmos11101049.

Lim, S.Y., Marzin, C., Xavier, P., Chang, C.P., Timbal, B., 2017. Impacts of boreal winter monsoon cold surges and the interaction with MJO on southeast Asia rainfall. J. Clim. 30, 4267–4281. https://doi.org/10.1175/JCLI-D-16-0546.1.

Lu, J., Li, T., Wang, L., 2019. Precipitation diurnal cycle over the Maritime Continent modulated by the MJO. Clim. Dyn. 53, 6489–6501. https://doi.org/10.1007/s00382-019-04941-8.

Madden, R.A., Julian, P.R., 1972. Description of global-scale circulation cells in the tropics with a 40–50 day period. J. Atmos. Sci. https://doi.org/10.1175/1520-0469(1972)029<1109:DOGSCC>2.0.CO;2.

Marzuki, M., Yusnaini, H., Ramadhan, R., Muharsyah, R., Vonnisa, M., Harmadi, H., Tangang, F., 2024. Diurnal cycle of precipitation over coastal sea and small islands in the eastern region of Sumatra including season and Madden Julian Oscillation signatures. Atmos. Res. 299, 107180. https://doi.org/10.1016/j.atmosres.2023.107180.

Oh, J.-.H., Kim, K.-.Y., Lim, G.-.H., 2012. Impact of MJO on the diurnal cycle of rainfall over the western Maritime Continent in the austral summer. Clim. Dyn. 38, 1167–1180. https://doi.org/10.1007/s00382-011-1237-4.

Qian, J.H., 2008. Why precipitation is mostly concentrated over islands in the maritime continent. J. Atmos. Sci. 65, 1428–1441. https://doi.org/10.1175/2007JAS2422.1.

Qian, J.H., 2020. Mechanisms for the dipolar patterns of rainfall variability over large islands in the maritime continent associated with the Madden-Julian oscillation. J. Atmos. Sci. 77, 2257–2278. https://doi.org/10.1175/JAS-D-19-0091.1.

Qian, J.H., Robertson, A.W., Moron, V., 2013. Diurnal cycle in different weather regimes and rainfall variability over borneo associated with ENSO. J. Clim. 26, 1772–1790. https://doi.org/10.1175/JCLI-D-12-00178.1.

Rauniyar, S.P., Walsh, K.J.E., 2011. Scale interaction of the diurnal cycle of rainfall over the Maritime Continent and Australia: influence of the MJO. J. Clim. 24, 325–348. https://doi.org/10.1175/2010JCLI3673.1.

Tan, H., Ray, P., Barrett, B., Dudhia, J., Moncrieff, M., Zhang, L., Zermeno-Diaz, D., 2022. Understanding the role of topography on the diurnal cycle of precipitation in the Maritime Continent during MJO propagation. Clim. Dyn. 58, 3003–3019. https://doi.org/10.1007/s00382-021-06085-0.

Wang, B., Rui, H., 1990. Synoptic climatology of transient tropical intraseasonal convection anomalies: 1975-1985. Meteorog. Atmos. Phys. 61, 43–61.

Wang, L., Li, T., Nasuno, T., 2018. Impact of Rossby and Kelvin wave components on MJO eastward propagation. J. Clim. 31, 6913–6931. https://doi.org/10.1175/JCLI-D-17-0749.1.

Wheeler, M.C., Hendon, H.H., 2004. An all-season real-time multivariate MJO index: development of an index for monitoring and prediction. Mon. Weather Rev. 132, 1917–1932. https://doi.org/10.1175/1520-0493(2004)132<1917:AARMMI>2.0.CO;2.

Wilks, D.S., 2011. Statistical Methods in the Atmospheric Sciences, 3rd ed. International Geophysics.

Zelinsky, R.C., Zhang, C., Liu, C., 2019. The relationship between the ITCZ and MJO initiation over the Indian Ocean. J. Atmos. Sci. 76, 2275–2294. https://doi.org/10.1175/JAS-D-18-0327.1.

Zhang, C., Dong, M., 2004. Seasonality in the Madden-Julian oscillation. J. Clim. 17, 3169–3180. https://doi.org/10.1175/1520-0442(2004)017<3169:SITMO>2.0.CO;2.

Zhang, C., Ling, J., 2017. Barrier effect of the Indo-Pacific Maritime continent on the MJO: perspectives from tracking MJO precipitation. J. Clim. 30, 3439–3459. https://doi.org/10.1175/JCLI-D-16-0614.1.

Zhou, Y., Wang, S., Fang, J., 2022. Diurnal cycle and dipolar pattern of precipitation over Borneo during an MJO event: Lee convergence and offshore-propagation. J. Atmos. Sci. 79, 2145–2169. https://doi.org/10.1175/JAS-D-21-0258.1.

Zhu, Y., Li, T., 2023. Characteristics of diurnal condensational heating at the Western Maritime Continent during MJO eastward propagation. Clim. Dyn. https://doi.org/10.1007/s00382-023-06761-3.